

BEAM INSTRUMENTATION PERFORMANCE DURING COMMISSIONING OF THE ESS RFQ, MEBT, AND DTL

T. J. Shea, R. A. Baron, C. S. Derrez, E. M. Donegani, V. Grishin, H. Hassanzadegan, I. Dolenc Kittelmann, H. Kocevar, N. Milas, D. Noll, H. A. Silva, R. Tarkeshian, C. Thomas, European Spallation Source ERIC, Lund, Sweden
 T. Papaevangelou, L. Segui, CEA-IRFU, Gif-sur-Yvette, France
 I. Bustinduy, ESS Bilbao, Zamudio, Spain
 M. Ferianis, Elettra-Sincrotrone Trieste S.C.p.A., Basovizza, Italy

Abstract

In late 2021 through mid 2022, the first protons were accelerated and transported through the European Spallation Source (ESS) Radio Frequency Quadrupole and Medium Energy Transport line at 3.6 MeV, and finally through the first Drift Tube Linac tank at 21 MeV. To enable these achievements, the following beam instrumentation systems were deployed: Ion Source power supply monitors, beam chopping systems, Faraday Cups, Beam Current Monitors (BCM) and Beam Position Monitors (BPM) that also measured phase. Additional systems were deployed for dedicated studies, including Wire Scanners, a slit and grid Emittance Measurement Unit, neutron Beam Loss Monitors and fast BCM and BPM systems. The instrumentation deployment is the culmination of efforts by a partnership of the ESS beam diagnostics section, multiple ESS groups and institutes across the globe. This paper summarizes the beam tests that characterized the performance of the instrumentation systems and verified the achievement of commissioning goals.

INTRODUCTION

Five weeks at the end of 2021 and several more weeks in early 2022 were dedicated to commissioning of the ESS Radio Frequency Quadrupole (RFQ) and Medium Energy Beam Transport line (MEBT) up to a Faraday Cup (FC) located in MEBT. After chopping in the Low Energy Beam Transport line (LEBT) and successful acceleration in the RFQ, the proton beam energy was 3.6 MeV. During June and July of 2022, several more weeks were dedicated to commissioning through the first Drift Tube Linac (DTL) tank with 21 MeV protons transported to a shielded FC. To support commissioning, the instrumentation systems were deployed in each linac section as depicted in Fig. 1. Most were designed to measure beam pulses pulses 5 to 50 μ s long with peak current ranging from 6 to 80 mA. This paper focuses on the instrumentation performance that underlies the commissioning results reported in overview papers [1–3].

The ESS beam instrumentation suite includes a wide variety of systems [4] deployed in a staged approach. Systems that are critical for meeting commissioning goals are verified in the laboratory prior to deployment, tested again with other systems in the accelerator environment and then formally verified with beam to achieve operational status. The Faraday

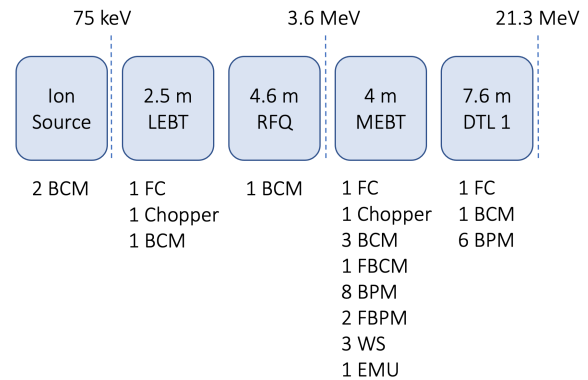


Figure 1: Layout of the linac sections and the beam instrumentation used during the 2021 and 2022 commissioning runs.

Cup (FC), Beam Current Monitor (BCM), Beam Position Monitor (BPM) and Chopper systems have all gone through this workflow. In addition, several other systems were verified for diagnostic beam studies with intent of gaining early experience with beam, sometimes at an intermediate stage of system development. For the recent commissioning runs, the neutron Beam Loss Monitors (nBLM), Wire Scanners (WS) and Emittance Measurement Unit (EMU) were deployed at this level and provided valuable data for the dual purposes of system development and beam characterization.

BEAM ACCOUNTING

Current Measurements

Six BCMs and three FCs measured the peak beam current that ranged from below 1 mA to beyond the nominal current of 62.5 mA. Figure 2 shows the proton current measured by the BCMs in each of the linac sections, as well as by the FC which was the beam destination at the end of the DTL1. An additional BCM channel also measured the 6 ms pulse extracted from the ion source and this is shown in the inner plot of Fig. 2. The few mA difference between the DTL1 BCM and the DTL1 FC flat top current are due to at least three reasons. Firstly, the DTL1 FC has an entrance foil that filters protons below the nominal energy; secondly, the electron repeller of the DTL1 FC was off; thirdly, the beam is expanded while travelling through the one meter long pipe connecting the DTL1 tank to the shielded beam

destination. The different starting times (shorter than 1 μs) between the rising edges of waveforms reflects the time of flight of the beam and the response time of the electronics. The ringing in the DTL1 FC waveform results from the combined frequency response of the FC electronics and the 40 meter signal cable.

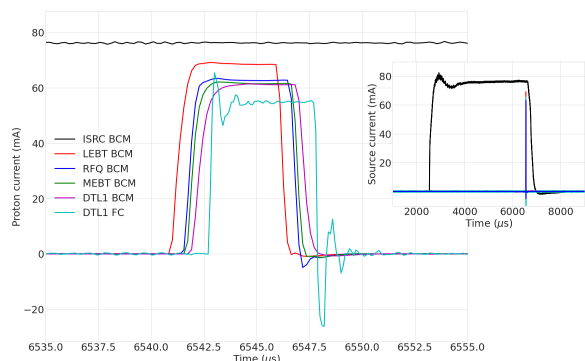


Figure 2: **Main plot:** The 5 μs long proton pulses measured by the BCMs and the DTL1 FC. **Inner plot:** zoom out showing the ms long proton pulse produced by the Ion Source, together with the 5 μs chopped pulse propagated along the accelerator.

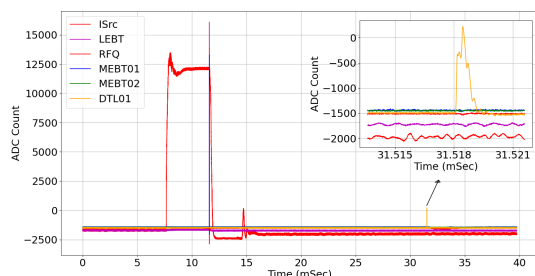


Figure 3: DTL BCM postmortem data showing a spike 20 ms after the beam pulse. The upper right plot shows the spike in more detail.

Machine Protection Functions

The BCM system also provides functions that protect the accelerator from beam-induced damage [5]. To assure the integrity of these functions as well as that of the normal beam characterization functions, the system was verified and calibrated to an accuracy better than the required ± 0.8 mA. The system has also demonstrated 0.01 mA precision and 0.1% linearity [6]. Implemented in a field-programmable gate array, the protection functions continuously monitor the current signal and via an interlock system will suppress beam production within 10 μs after detecting an errant condition. Errant conditions include beam detected above a current limit or outside a time window. After verification with beam, these protection functions were relied upon throughout commissioning. Due to the varying conditions during commissioning as well as parallel activities such as radio-frequency

(RF) conditioning of the DTL, additional signals challenged the protection functions and led to false trips. An example is shown in Fig. 3. In the DTL BCM, a short spike of current is measured outside the desired time window, an errant condition that led to an interlock. The spike was detected after the DTL when the destination was the MEBT FC, and hence no beam was transported through the DTL. During this time, the DTL tank was being conditioned, so electrons or ions resulting from this process are suspected to be the source of the spike.

Neutron Measurements

The neutron beam loss monitor system [7] was deployed for studies and successfully measured the first neutrons produced as a result of intentional beam loss. In the study, 20 μs proton pulses with an energy of 3.6 MeV and a peak current of about 60 mA were steered onto a chopper dump made of the molybdenum alloy TZM. The sub- μs time structure displayed in Fig. 4 illustrates the fast nBLM detector's intra-pulse measurement capability.

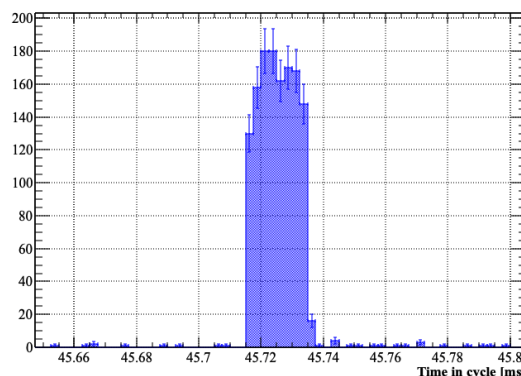


Figure 4: Neutrons detected by the fast nBLM.

CENTROID MEASUREMENTS

The BPMs in the MEBT and DTL measure the transverse position and the phase of the bunch centroids. The MEBT section has been designed with 7 stripline BPMs and an additional BPM to perform time domain characterization of the beam. In the first DTL tank, 6 shorted stripline BPMs are embedded in drift tubes. [8]

In the MEBT only, a so-called fast BPM system performs wide bandwidth characterization of the beam. This system uses regular BPM stripline sensors serviced by a separate 5 GHz bandwidth, 20 GSa/s acquisition system. Calibrated RF chains tap the signals from 2 BPMs spaced 30.1 cm apart. To minimize the measurement error, cables, RF couplers and RF amplifiers have been trimmed to have less than tens of picoseconds propagation delay difference. This system has measured the RFQ output energy, LEBT Chopper vs MEBT Chopper timing alignment, and the beam's general bunching structure. The signal acquisition bandwidth is currently limited by the response of the stripline sensors to the low-velocity protons.

Content from this work may be used under the terms of the CC BY 4.0 licence (© 2022). Any distribution of this work must maintain attribution to the author(s), title of the work, publisher, and DOI

Beam Position

BPMs were typically used during commissioning to perform lattice characterization. Raw waveforms, decimated waveforms and scaler data (1 point per pulse) are available for characterization of the machine and its beam properties. Figure 5 demonstrates a typical example of a beam steering study. In this sequence of waveforms, the ability to measure position variation within the short pulse is evident.

The beam position fluctuations versus beam current have been measured by acquiring position data in the MEBT while varying the iris aperture in the LEBT. Figure 6 shows the the evolution of the beam current and standard deviation of the position measurement during this scan.

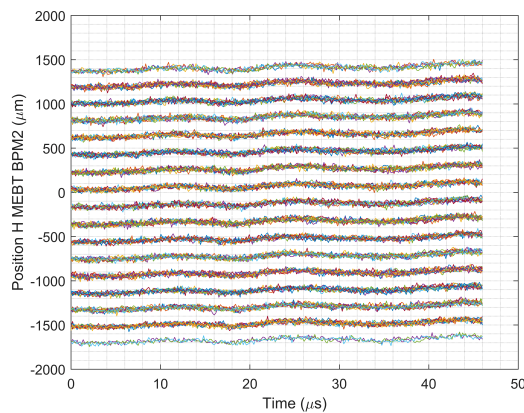


Figure 5: Typical intra-pulse position measurements for a 50 μs pulse and 6 mA beam during a beam steering characterization. Each waveform on the plot corresponds to a pulse acquisition for a specific beam position, adjusted by the MEBT correctors.

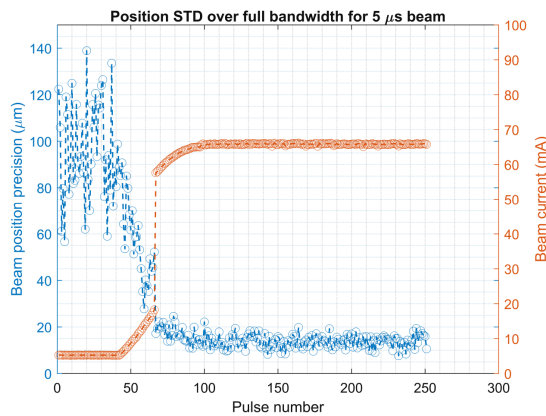


Figure 6: Beam position resolution vs. the beam current for a 5 μs pulse. The plot demonstrates the position measurements standard deviation, which in this case is dominated by the beam fluctuations.

Beam Phase

Phase scans were the primary technique used to tune the MEBT bunchers and the DTL tank. During these scans, the amplitude and phase difference between BPMs are monitored. To avoid interference from the fundamental RF frequency, MEBT and DTL BPMs are tuned to the second harmonic of the beam, making them particularly sensitive to bunch length variations which then results in a strong signature of the optimal RF phase setpoint. A typical plot showing the amplitude and phase difference is presented in Fig. 7.

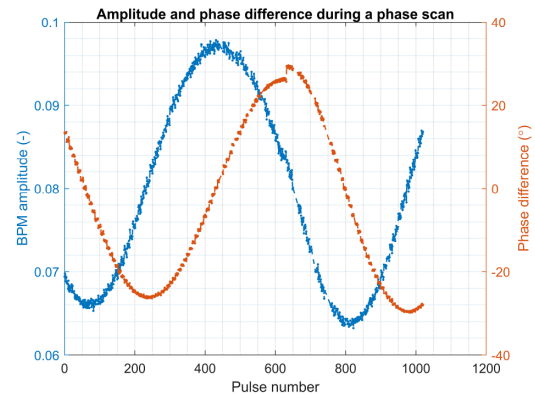


Figure 7: Typical phase scan data from the BPM for a 5 μs pulse length and 5.2 mA beam current. BPM 3 amplitude and phase difference between BPM 3 and 5 are shown on this plot.

Absolute beam energy measurements were performed with the fast BPM system by measuring the absolute time of flight between the two BPM sensors. The measurements over approximately one hour are shown in Fig. 8. Time domain measurements and the distribution are also presented.

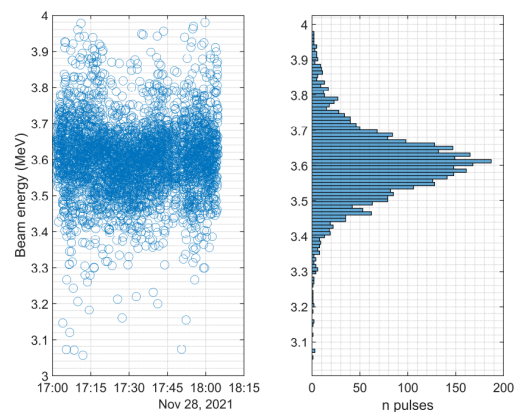


Figure 8: Time domain and energy distribution measurements over approximately one hour of machine operation as measured by the fast BPM.

DISTRIBUTION MEASUREMENTS

Wire Scans

The three MEBT WS stations on the beam line are a delivery from ESS Bilbao, while the full acquisition chain is an in-kind contribution from Elettra Sincrotrone Trieste in Italy. Secondary emission electrons provide the signal from 33 micron carbon wires. Horizontal and vertical wires are mounted on a single actuator that scans at a 45 degree angle from horizontal. Key specifications of the system include a time resolution of 1 μ s, an accuracy of 0.1 mm and a dynamic range of 10^3 . The system performance can be assessed after running through the verification process that includes a check of wire integrity, optimization of the bias voltage, and setting of the acquisition and motion parameters including scanning speeds, modes, gains and ranges [9]. Once these initial performance assessments were completed, the systems were further tested using high level data evaluation tools. Typical scan results with beam are depicted in Fig. 9.

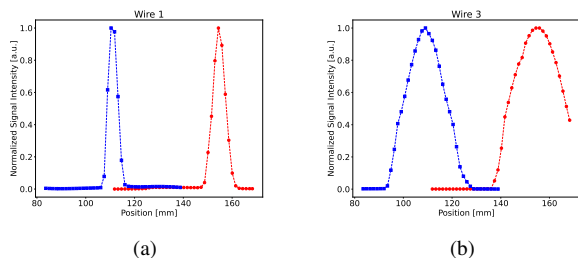


Figure 9: Raw scan results for the first (a) and last (b) wire scanners upstream of the MEBT Faraday Cup.

Emittance Scans

Developed as a collaboration between ESS in Lund and ESS Bilbao, the MEBT EMU consists of a slit with a 0.1 mm aperture followed by a wire grid 368 mm downstream. The wires in the grid are 35 microns in diameter and spaced 0.5 mm apart. Additional bias wires control the field seen by the secondary emission electrons, and during initial beam studies, the bias voltage was increased until it stopped affecting the signal. Following configurable gain stages, 5 MSa/s digitizers simultaneously acquire all 24 grid signals. Early in the beam tests, noise from the grid motor drivers was observed on these signals, so the scan software was modified to de-energize the drivers during signal acquisition. This enabled a measurement precision of about ± 2 nA in a 200 kHz bandwidth.

After setting up the bias and the signal acquisition parameters, the focus turned to optimization of the scanning parameters. Figure 10 shows a typical scanning result, combining 8 separate scans of the slit. At each grid position, the slit position was scanned in steps of 0.5 mm. The angular resolution of the measurement was improved by taking multiple measurements at grid positions displaced by a fraction of the wire pitch. The angular range was increased by taking

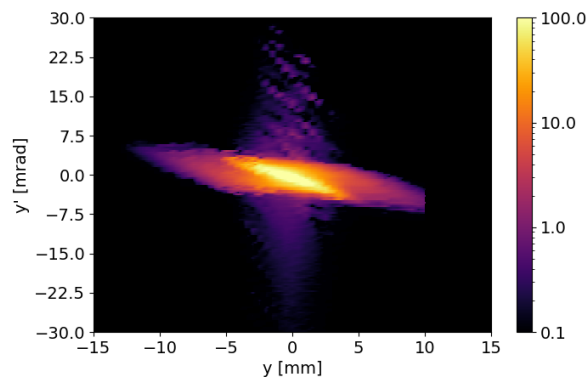


Figure 10: Phase-space measurement using the slit grid emittance scanner. The vertical phase space distribution is shown with a logarithmic intensity scale.

multiple sets of measurements with the grid displaced by its total size.

A specific, special beam optic was used for the EMU measurement with the goal of producing a large and divergent beam. The measurement shows a strong beam core with ± 5 mm size surrounded by a halo of yet-to-be-determined origin. The low-level signal at $|y'| > 7.5$ mrad around the beam core is assumed to be an artifact of the measurement – all signals disappear when the grid is moved to a position where the core of the beam misses the grid entirely. This data is being further analyzed for better understanding of the performance of the device and the beam optics.

OUTLOOK

All systems required for commissioning were verified and available for first protons. High level performance requirements were met and with some limitations, all of these systems were declared operational. In addition, several instruments were prepared for studies and acquired beam data for the first time. Operational experience revealed the need for some improvements that are underway in preparation for the next commissioning run. This upcoming run, currently scheduled for Spring/Summer of 2023 will take beam through the first 4 of 5 DTL tanks to about 70 MeV.

ACKNOWLEDGEMENTS

The authors appreciate the critical efforts of the many diagnostics and controls team members that brought these instrumentation systems to life. We also thank the operations and commissioning teams that devoted extended hours to beam tuning, studies and data acquisition.

REFERENCES

- [1] R. Miyamoto *et al.*, “Beam Commissioning of Normal Conducting Part and Status of ESS Project,” presented at LINAC’22, Liverpool, UK, Aug.-Sep. 2022, paper MO1PA02, to be published.

- [2] N. Milas, M. Eshraqi, Y. Levinsen, R. Miyamoto, and D. Noll, “Beam Tuning Studies in the ESS MEBT,” presented at IBIC’22, Krakow, Poland, Sep. 2022, paper MO2C2, this conference.
- [3] Y. Levinsen *et al.*, “First RF Phase Scans in the European Spallation Source,” presented at IBIC’22, Krakow, Poland, Sep. 2022, paper TUP35, this conference.
- [4] T. J. Shea *et al.*, “Overview and Status of Diagnostics for the ESS Project,” in *Proc. IBIC’17*, Grand Rapids, MI, USA, Aug. 2017, pp. 8–15.
doi:10.18429/JACoW-IBIC2017-MO2AB2
- [5] H. Hassanzadegan *et al.*, “Machine Protection Features of the ESS Beam Current Monitor System,” in *Proc. IPAC’18*, Vancouver, Canada, Apr.-May 2018, pp. 2058–2060.
doi:10.18429/JACoW-IPAC2018-WEPAF088
- [6] H. Hassanzadegan *et al.*, “Beam Current Monitor System of the European Spallation Source,” in *Proc. LINAC’14*, Geneva, Switzerland, Aug.-Sep. 2014, 526–528.
<https://jacow.org/LINAC2014/papers/TUPP041.pdf>
- [7] I. Dolenc Kittelmann *et al.*, “Neutron sensitive beam loss monitoring system for the European Spallation Source linac,” *Phys. Rev. Accel. Beams*, vol. 25, p. 022 802, 2022.
doi:10.1103/PhysRevAccelBeams.25.022802
- [8] R. A. Baron *et al.*, “ESS Beam Position and Phase Monitor System,” in *Proc. IBIC’19*, Malmö, Sweden, Sep. 2019, pp. 543–547. doi:10.18429/JACoW-IBIC2019-WEPP015
- [9] C. S. Derrez *et al.*, “Wire Scanner Systems at the European Spallation Source (ESS): Tests and First Beam Commissioning Results,” presented at LINAC’22, Liverpool, UK, Aug.-Sep. 2022, paper TUPOJO13, unpublished, 2022.